JOURNAL OF CATALYSIS 130, 293–305 (1991)

AlNbO Oxides as New Supports for Hydrocarbon Oxidation

I. Preparation and Characterization of the Support

P. G. PRIES DE OLIVEIRA,* F. LEFEBVRE,† M. PRIMET,† J. G. EON,‡ AND J. C. VOLTA†

*Instituto Nacional de Tecnologia, Avenida Venezuela 82, Praça Maua, 20081, Rio de Janeiro, Brasil; †Institut de Recherches sur la Catalyse, CNRS, 2 Avenue A. Einstein, 69626, Villeurbanne Cédex, France; and ‡Instituto Militar de Engenharia, Praça General Tiburcio 80, Urca, 22290, Rio de Janeiro, Brasil

Received November 1, 1990; revised January 29, 1991

Al–Nb oxides were prepared from niobium and aluminum oxalates in aqueous solution and calcined at temperatures ranging from 500 to 820°C. X-ray diffraction and ^{27}Al MAS NMR showed the crystallization into $AlNbO_4$ at about 750°C. FTIR studies showed the presence of different surface hydroxyl groups; their concentration was measured from MS–TGA experiments. The Al–Nb oxides were tested for isopropanol dehydration. It was observed that the turnover number increases with the temperature of the treatment. The concentration and the nature of the hydroxyl groups are discussed in relation with the structure of the solids.

INTRODUCTION

Many studies have been devoted to the control of the catalytic properties of vanadium and molybdenum oxides catalysts by the dispersion of these elements on oxide supports like alumina, silica, and titania (*1*). The vanadia–titania system was the subject of many studies on olefins, aromatics, and alkylaromatics oxidation (*2*). The famous example of the specificity of the V/TiO_2 (anatase) system for O-xylene oxidation to phthalic anhydride (PA) is well known (*3–5*). It has been proposed that the structural isomorphism between V_2O_5 and TiO_2 (anatase) is responsible for the improvement to PA yield (*6–9*). This aspect must be related to the concept of a structural induction of the active phase by the support which is now well admitted (*10, 11*). At low coverage, in a domain near the so-called "monolayer," the catalytic properties appear to be improved (*3, 12*).

Indeed, the support can induce specific characteristics of the active sites, taking into account both its structural and its acido-basic features. Aluminum niobate, $AlNbO_4$, which crystallizes in the monoclinic system (*13*), presents a structure similar to that of TiO_2 (B) (*14*). A promoting effect of V_2O_5 has been observed for both these supports (*10*). The presence of Al and Nb with different acido-basic properties was suspected to be of interest in control of the superficial properties of the $AlNbO_4$ support and thus in the inducement of a specific grafting ability of VO_x species onto $AlNbO_4$ in the domain of the "monolayer."

This article describes the conditions of preparation of the $AlNbO_4$ support and a physicochemical study of this material according to the temperature of calcination. The reaction of dehydration of isopropanol was used in order to evaluate the acido-basic properties of the AlNbO oxides. A correlation between the catalytic activity, the nature, and the concentration of the superficial hydroxyl groups is attempted. In a future article, a catalytic study of VO_x/AlNbO oxides will be presented (*15*).

EXPERIMENTAL

AlNbO oxides were prepared from $Al(NO_3)_3$, 9 H_2O, and from the niobium complex NH_4, $H_2(NbO(C_2O_4)_3)$, x H_2O pro-

0021-9517/91 $3.00

TABLE 1

Scheme for Preparation of AlNbO Oxides

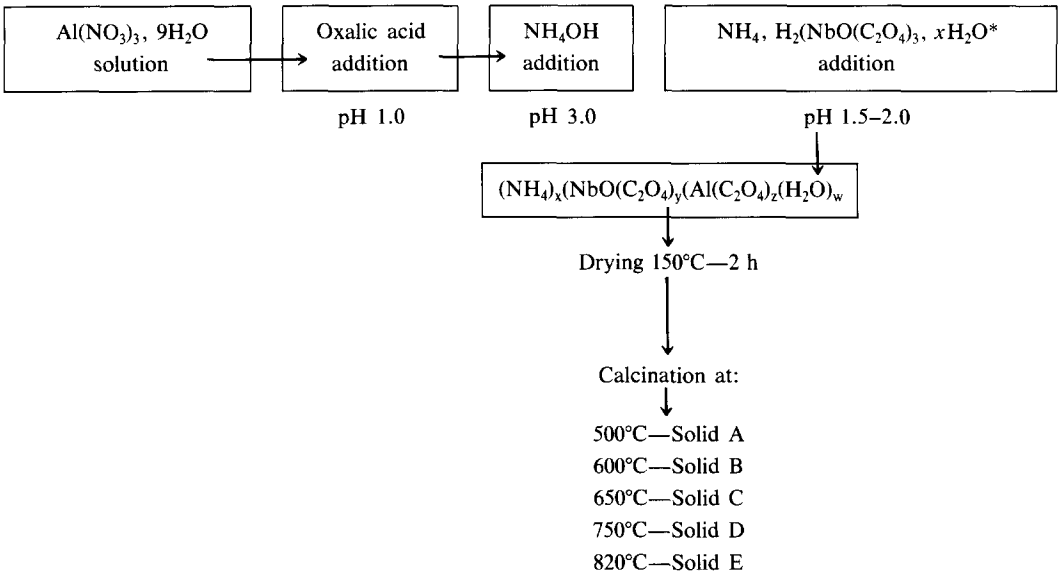

* Formula proposed by CBMM Co (Companhia Brasileira de Metalurgia e Mineração).

duced by CBMM (Companhia Brasileira de Metalurgia e Mineração). $Al(NO_3)_3$, 9 H_2O was dissolved in aqueous solution and then oxalic acid and ammonia were successively added until a pH of 1.0 and 3.0, respectively, was reached (see Table 1). After 15 min of stirring, the niobium complex was added with a ratio Al/Nb = 1.0 (pH 1.5). The slightly blue solution was refluxed for 1 h. Water was then removed under vacuum. The white paste obtained was dried at 150°C for 15 h. This material, called P_{AlNb}, was the precursor of the AlNbO oxides. Five solids were prepared by calcination under a flow of air of P_{AlNb} at 500°C (Solid A), 600°C (Solid B), 650°C (Solid C), 750°C (Solid D), and 820°C (Solid E), respectively. Al and Nb precursors (P_{Al} and P_{Nb}) were prepared with the same procedures.

For chemical analysis, solids were primarily solubilized in a HF/HCl solution. Al and Nb contents of the final solids were determined by atomic absorption for Al and by atomic emission for Nb.

Precursors were examined by infrared spectroscopy using a Perkin–Elmer 580 in the 4000–400 cm^{-1} region. Solids were mixed with KBr (1%) and pressed into a thin wafer. Decomposition of the precursors was studied by DTA–TGA analysis using respectively a MDTA 85 SETARAM microanalyzer and a 4102 SARTORIUS microbalance. Studies were conducted under air flow (3.6 liter h^{-1}) with a linear increase of the temperature (2°C/min) in the 25–850°C region.

The structure of the AlNbO oxides was identified by X-ray diffraction using a Siemens diffractometer with the Cu$K\alpha$ radiation in the 0–75° 2Θ domain, and by ^{27}Al solid-state MAS NMR spectroscopy. Spectra were recorded on a Bruker MSL-300 spectrometer by using a single pulse sequence. Conditions were chosen in order to obtain quantitative spectra (small pulse angle, long delay between the pulses) and all the samples were spun at the magic angle with the same frequency (3000 Hz). Chemical shifts were referred to $Al(H_2O)_{6aq}^{3+}$.

Textural measurements were performed

on an automatic apparatus home made at IRC (area and porosity determination).

For XPS measurements, samples were introduced into a Hewlett–Packard HP 5950 A spectrometer and outgassed at room temperature to a pressure of 10^{-9} Torr. The spectrometer was monitored by a computer and the different spectra were accumulated from 5 min to 2 h, depending on their intensity. The experimental spectra were treated by computer software for smoothing, substraction of the background, and determination of the peak areas. Binding energy values were referred to C 1*s* peak (pollution carbon) at 284.5 eV.

Electron microscopy investigation was undertaken using a Jeol 100C electron microscope in transmission mode. Microanalysis of the elemental composition of the solids (EDX) was carried out using a STEM (scanning transmission electron microscope) HB5 from vacuum generator. The identification of the surface hydroxyl groups was performed using a Fourier transform spectrometer (IFS 110 from Bruker) and signal accumulation in the 4000–1000 cm^{-1} range. Mass samples ranging from 8 to 30 mg were pressed into a thin wafer. They were outgassed at 150°C under 10^{-5} Torr into a quartz cell. Spectra were accumulated depending on the disk sample transparency. The determination of the hydroxyl groups concentration was done by coupling TGA (Sartorius 4102 thermobalance) and MS measurements (Quadrex 200 Inficon). Samples were previously outgassed at 200°C under 10^{-3} Torr for 16 h.

AlNbO oxides were compared for isopropanol dehydration in a flow system. The catalyst was deposited on a fixed bed in a Pyrex microreactor (U tube, 13 mm diameter) operating under atmospheric pressure. The catalytic zone was isothermal (m = 200 mg). Reaction temperature varied from 150 to 200°C. The isopropanol vapor pressure (P = 28 Torr) was controlled by a saturator condensor system with three vessels. Nitrogen was used as carrier gas. Analysis of reactants and reaction products was done by on-line gas chromatography. For the permanent gases, a Delsi/IGC 120MB gas chromatograph equipped with a thermal conductivity detector was used. Helium was the carrier gas (5.7 liter/h). O_2 and CO were separated on a 0.3 m × $\frac{1}{4}$ in. molecular sieve 5-Å column. For the organic products, a Delsi IGC 120 FB gas chromatograph equipped with a flame ionization detector was used. Nitrogen was the carrier gas. Propene and acetone were separated on a 1 m × $\frac{1}{8}$ in. Porapak Q column.

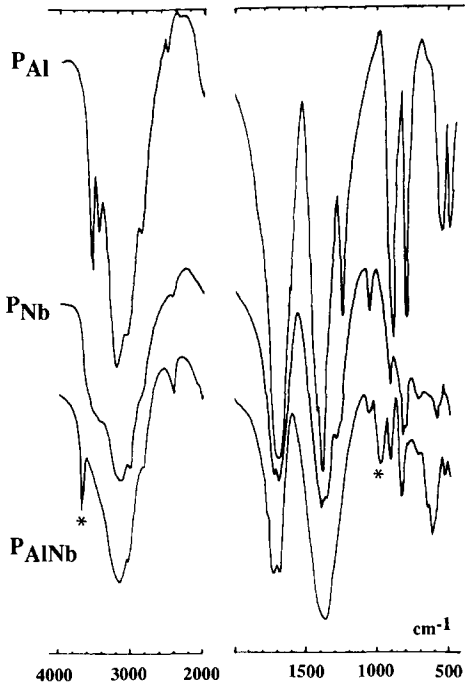

FIG. 1. Infrared spectra of the precursors (*characteristic bands of P_{AlNb}).

RESULTS

Solids Characterization

The infrared spectra of P_{Al}, P_{Nb}, and P_{AlNb} are given in Fig. 1. They present characteristic bands of oxalate complexes (*16, 17*). However, it is noteworthy that P_{AlNb} exhibits two bands at 970 and 3690 cm^{-1} which are not present in P_{Al} and P_{Nb}. This could be indicative of an interaction between the two elements of the precursor.

Curves obtained by DTA–TGA analysis during the decomposition of the three pre-

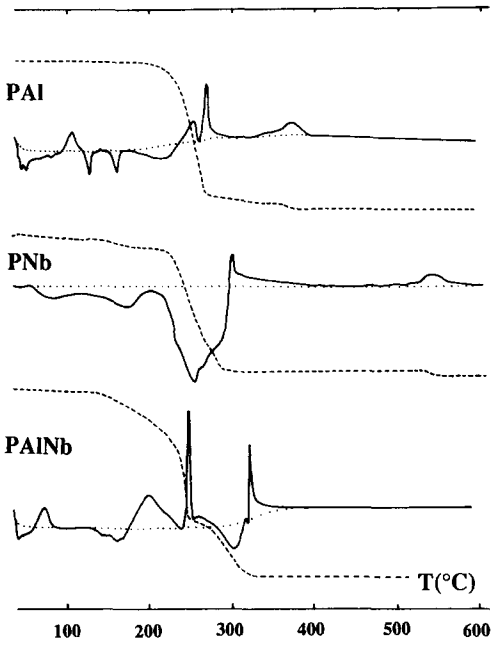

FIG. 2. DTA–TGA curves of the decomposition of the precursors — DTA; --- TGA; ↑ exo; ↓ endo; P_{Al}: m = 48.7 mg; P_{Nb}: m = 54.4 mg; P_{AlNb}: m = 66.2 mg.

cursors are given in Fig. 2. Decomposition of P_{Al} begins at 200°C when it starts at lower temperatures for P_{Nb} (50°C) and for P_{AlNb} (150°C). It is practically impossible to separate the decomposition of the oxalate complex from NH_3 elimination for P_{Al} and P_{Nb} in the 200–300°C region. The large exothermic peaks observed between 334 and 400°C for P_{Al} and around 530°C for P_{Nb}, with little weight loss, may be ascribed to CO_2 evolution from the materials (*17*) or to crystallization of the oxides. The events which occur during the decomposition of P_{AlNb} can be easily interpreted taking into account the decomposition of P_{Al} and P_{Nb} separately. It appears that the emission of H_2O bound to Nb starts the decomposition (endothermic peak at 130–160°C) and is followed by the decomposition of the Al oxalate complex, and finally, after a pseudoplateau on the TGA curve at 260°C, is followed by the decomposition of the Nb oxalate complex. It is noteworthy that both the position and the form of the DTA peak of the last phenomenon are modified in comparison with P_{Nb} confirming the retarding effect played by the presence of Al in the structure of P_{AlNb}. The final decomposition of P_{AlNb} which occurs at 350°C ends with the interaction between both structures of Al and Nb and the hypothetic formation of a new AlNbO material, due to the absence of any peak characteristic of the crystallization of Al_2O_3 and Nb_2O_5. An exothermic peak which was irreversible was observed at 790°C. It is not presented in Fig. 2.

Figure 3 shows the evolution of the texture of the AlNbO oxides with the calcination temperature. BET area decreases regularly from 168 m^2/g for Solid A calcined at 500°C to 53 m^2/g for Solid D calcined at 750°C. Simultaneously a displacement of the maximum of the porosity was observed from 3 nm for Solids A and B to 4.5 and 5.5 nm respectively for Solids C and D.

The X-ray diffraction pattern of the AlNbO oxides presented in Fig. 4 shows that crystallization into $AlNbO_4$ occurs for Solid D. The diffraction spectrum observed for this solid is quite in agreement with the cor-

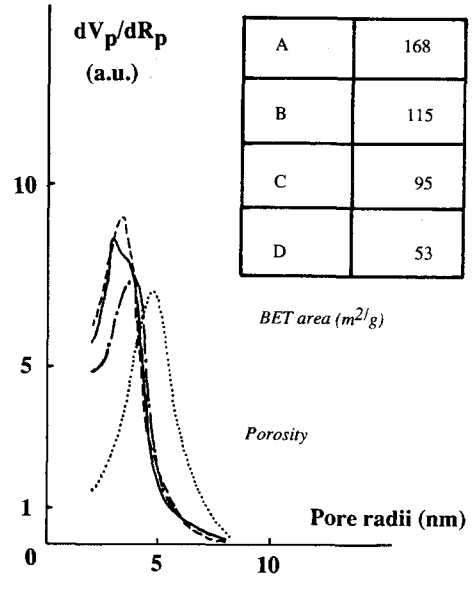

FIG. 3. Evolution of the texture of the AlNbO oxides with the calcination temperature: —A ----B –·–C ·····D.

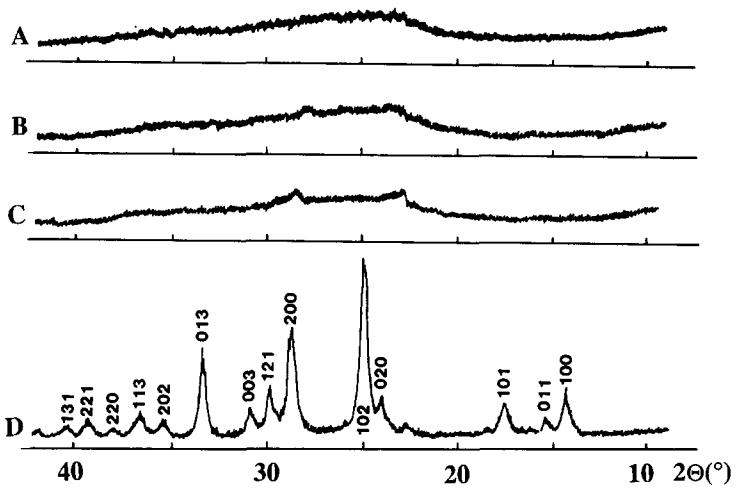

FIG. 4. Powder X-ray diffraction pattern of the AlNbO oxides.

responding ASTM file (*18*). The same spectrum was observed for Solid E. As a consequence, the exothermic effect previously observed by DTA at 790°C, temperature between 750 (preparation of Solid D) and 820°C (preparation of Solid E) was attributed to the crystallization of the aluminum niobate. The indexing of the diffraction patterns of Solids A, B, and C appears more difficult. Solids A, B, and C are poorly crystallized. However, two peaks are observed at 23 and 28° (2Θ) which can be respectively attributed to the (101) and (008) lines of Nb_2O_5 (*19*).

The ^{27}Al MAS NMR study of the corresponding solids confirmed the evolution of the structure of the materials by increasing the temperature of calcination from 500 to 750°C (*20*). The spectrum of Solid D (Fig. 5d) obtained by calcination at 750°C, the temperature which corresponds to that of crystallization of $AlNbO_4$ as previously observed by XRD, shows only one peak at -1.8 ppm, which can be attributed to octahedral aluminum, in agreement with the structure of $AlNbO_4$ as published by Pedersen (*13*) (see Fig. 13). For Solids A, B, and C obtained at lower calcination temperatures the ^{27}Al spectra (Fig. 5a, 5b, and 5c) are more complex, and at least three peaks at about 0, 30, and 60 ppm can be detected. The signal at 0–2 ppm is attributed to aluminum in the same octahedral environment as in the crystalline $AlNbO_4$ phase, while the peak at 58–60 ppm corresponds to tetrahedral aluminum as in zeolites (*21*). The attribution of the signal at 28–30 ppm is more controversial and depending on the authors it is attributed to pentacoordinated atoms or to aluminum in a tetrahedrally distorted coordination (*21–24*).

Figure 6 presents a photograph of Solid D corresponding to crystallized $AlNbO_4$. A STEM examination of the same sample showed an atomic Al/Nb ratio of 0.95 close to both the theoretical one and the value of 1.09 deducted from the chemical analysis.

In order to study the superficial properties of the AlNbO oxides as a function of the temperature of calcination two series of experiments were performed: a FTIR study of the hydroxyl groups, and a TGA–MS study in order to measure their number by desorption of the corresponding water. For both studies, precautions were taken to standardize the samples before each measurement.

For the FTIR study, experiments were conducted with Solid A which was pretreated in the IR cell under O_2 for 3 h at 500°C and then outgassed at 150°C under

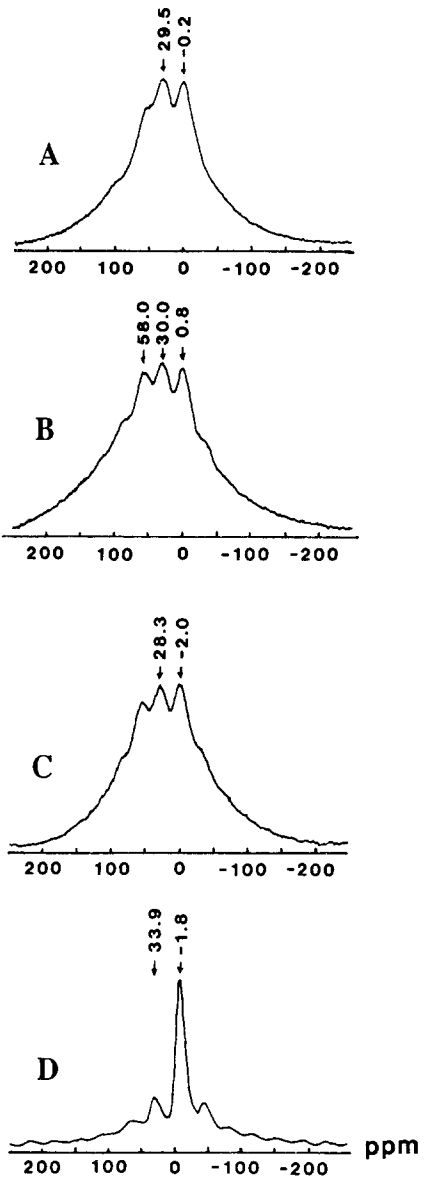

FIG. 5. ^{27}Al MAS NMR spectra of the AlNbO oxides (chemical shift referred to $Al(H_2O)_{6aq}^{3+}$).

a final pressure of 10^{-5} Torr to eliminate physisorbed water before IR examination at room temperature. The same procedure was performed for an oxygen treatment at 600°C (conditions of calcination of Solid B), 650°C (Solid C), and 750°C (Solid D). IR spectra are given in Fig. 7 in the 3300–3900 cm^{-1} region. Intense bands which are characteristic of the OH groups are observed for Solid A at 3820, 3730, 3690, 3580, 3485, 3410, and 3345 cm^{-1}; for Solid B at 3820, 3720–3690, 3580, 3485, 3410, and 3310 cm^{-1}; and for Solid C at 3820, 3700–3500, 3490, 3410, and 3345 cm^{-1}. Less intense bands are observed for Solid D, which corresponds to crystallized $AlNbO_4$ at 3825, 3680, 3500, and 3345 cm^{-1}. The assignment of the OH-stretching bands is discussed later.

The hydroxyl groups can be removed by condensation from two neighboring sites. This leads to the formation of a water molecule that is then expelled from the surface. Thus, the concentration of OH groups can be measured from evolved water by coupling TGA and MS after outgassing the samples at 200°C under low pressure in order to avoid any perturbation from physisorbed water. It was first observed that water is the main desorbed molecule, so that the weight loss as function of the desorption temperature was only indicative of water coming from the condensation of neighboring OH groups. The shape of the TGA curves for the desorption of Solids A, B, C, and D were similar, suggesting a continuity of their superficial properties. This result is in agreement with the continuity observed also for the FTIR spectra (Fig. 7). The total mass variation observed at the plateau near 800°C was used to measure the concentration of the OH groups. This is presented in Table 2. As normally expected, the OH density monotonously decreases with the calcination temperature and the subsequent BET area.

Figure 8 gives the O 1*s* photoemission peaks of Solids A and D. The occurrence of one or more high binding energy (BE) component(s) in the O 1*s* peaks is evident from a survey of the experimental profiles of oxides. The high BE signals are generally assigned to adsorbed H_2O or OH surface species, as observed in the case of TiO_2 (*25*). This was also the case of Nb_2O_5 (*26–28*) for which the principal O 1*s* peak at 529.8 eV

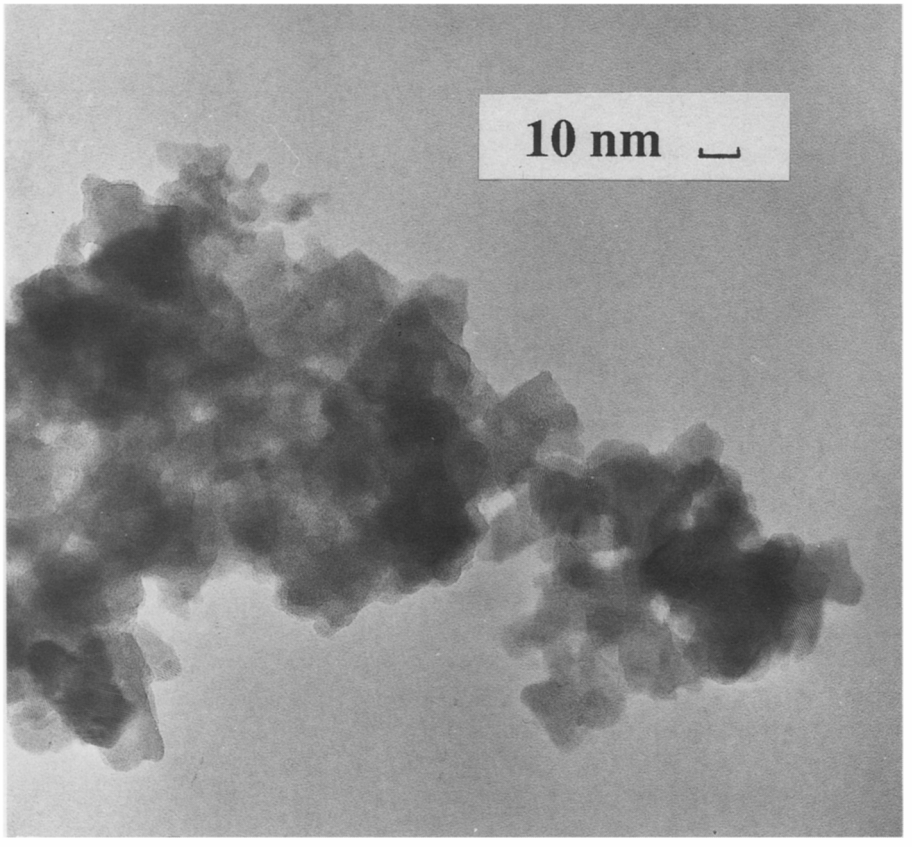

FIG. 6. TEM photograph of Solid D (magnitude 500,000).

was associated with a second peak at 532.2 eV ascribable to OH surface species. The O 1*s* peak of Al_2O_3 is currently observed at 531.8 eV and is also assigned to the OH surface species (*29, 30*). Let us consider first the O 1*s* spectrum of Solid D, the structure of which is $AlNbO_4$. A maximum is observed at 530.5 eV which is characteristic of $AlNbO_4$ oxygen atoms. Note that the spectrum is displaced toward high binding energy (532 eV), typical of OH surface species, which is indicative of a slight hydroxylation of this material. The spectrum of Solid A can be deconvoluted into two components using computer techniques with two maxima at 530.4 and 532.1 eV. The first peak is situated closer to 530.5 eV (characteristic of $AlNbO_4$—see previously) than to 529.8 eV (characteristic of Nb_2O_5) (*26–28*), which should be in favor of the superficial presence of $AlNbO_4$ and Nb_2O_5, but with a higher content of the first component. The superficial Al/O atomic ratio of 0.26 close to that of $AlNbO_4$ observed for Solid D (0.25) supports this hypothesis. The second peak observed at 532.1 eV is indicative of OH surface species existing on Al_2O_3, Nb_2O_5, and $AlNbO_4$. Figures 9 and 10 give the Nb $3d^{3/2}$–Nb $3d^{5/2}$ and Al 2*p* photoemission peaks respectively, for the same solids. Spectra are very similar for each family with a higher BE for Solid D. The experimental values may be compared with the BE of pure oxides observed respectively at 74.5 eV for the Al 2*p* peak and 207.6 eV for the Nb $3d^{5/2}$ peak (*27*). These two results are

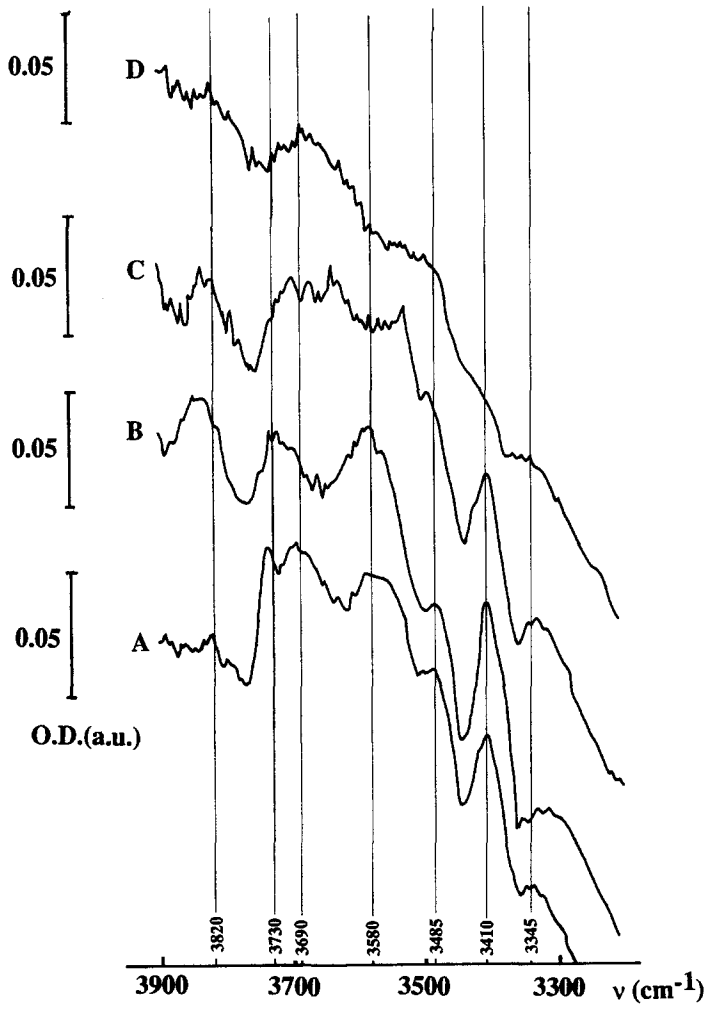

FIG. 7. FTIR spectra of the AlNbO oxides (referred to a sample mass of 26 mg).

TABLE 2

Density of Hydroxyl Groups

Solids	S_{BET} (m^2/g)	nOH/nm^2
A	168	2.11
B	115	1.97
C	95	1.50
D	53	0.93

Note. The determination of the OH groups concentration was done by coupling TGA and MS measurements. Samples were previously outgassed at T = 200°C; $P = 10^{-3}$ Torr for 16 h.

respectively indicative of the superficial presence of $AlNbO_4$ on both Solid A and D with a good crystallinity for Solid D.

Reaction Study

Catalytic dehydration of isopropanol was studied on the different AlNbO oxides. Propene was the only product detected with a good carbon balance (98%). The four solids did not give any acetone (indicative of a possible redox reaction) and CO or CO_2. These results suggest a mild acidic character for these materials. Figure 11 gives the propene yield as a function of the temperature for the same mass of catalyst (200 mg). The

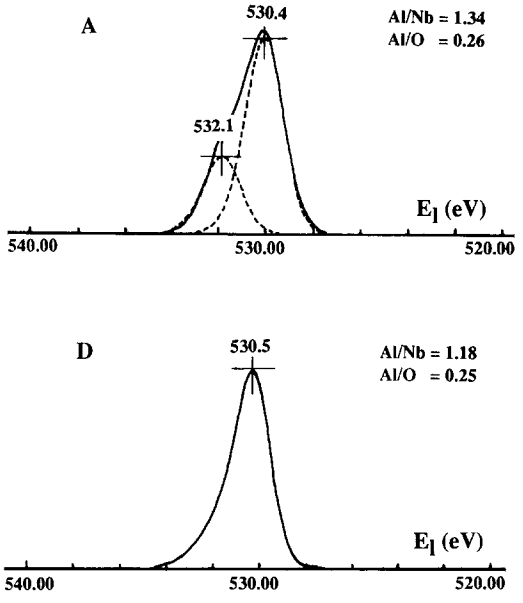

FIG. 8. XPS spectra of O 1*s* for AlNbO oxides A and D.

apparent activation energy was the same for the four solids, namely 20–21 kcal · mol^{-1}. At a given temperature, the yield increases from Solid D to Solid A. However, the calculated turnover number (TON) increases from Solid A to Solid D, suggesting the presence of proportionally more acidic hydroxyl catalytic sites for dehydration for the later. This is illustrated on Fig. 12, where it appears that TON decreases as the OH density increases.

DISCUSSION

AlNbO oxides have been prepared from niobium and aluminium oxalates precursors. Their calcination leads to AlNbO oxides, of which the structure and the superficial properties strongly depend on the temperature of calcination.

The DTA–TGA study shows a strong interaction between Al and Nb into the structure of the Al–Nb precursor so that during its decomposition, none of the crystalline Al_2O_3 and Nb_2O_5 structures have been identified by XRD in the 500–820°C temperature domain. This interaction is in agreement with the IR data of the precursors with the existence of new bands for the Al–Nb precursor.

The combination of XRD, ^{27}Al MAS NMR, XPS, and STEM leads us to conclude that the formation of crystalline $AlNbO_4$ is observed around 750°C. The normal octahedral coordination for aluminum is observed for this material (*13*) (see Fig. 13). Below this temperature, solids obtained are poorly crystallized and both XRD and ^{27}Al MAS NMR studies show some disorder with interaction between the two phases. These conclusions are supported by the FTIR study of superficial OH groups which shows, together with ν OH bands characteristic of Al_2O_3 and Nb_2O_5 structures, the presence of new ν OH bands issued from the perturbation of the absorption bands of OH groups of alumina by niobia and niobia by alumina, at short distance, as is further discussed.

The assignment of the OH-stretching bands on different oxides and especially on alumina seems still ambiguous (*31–35*). Very few studies were concerned with the

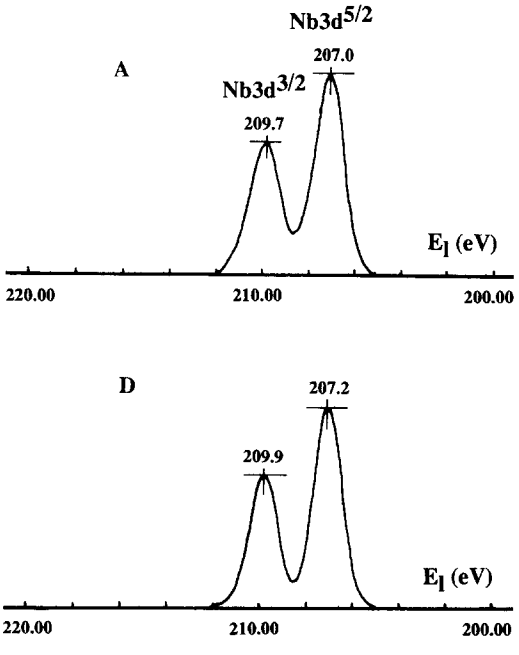

FIG. 9. XPS spectra of Nb $3d^{3/2}$ and $3d^{5/2}$ for AlNbO oxides A and D.

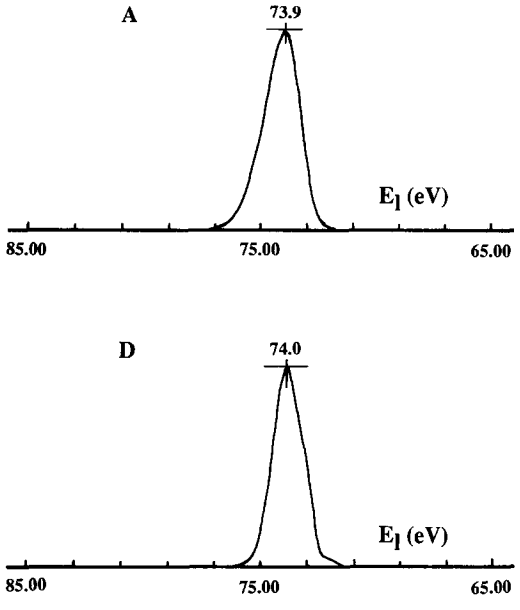

FIG. 10. XPS spectra of Al 2*p* for AlNbO oxides A and D.

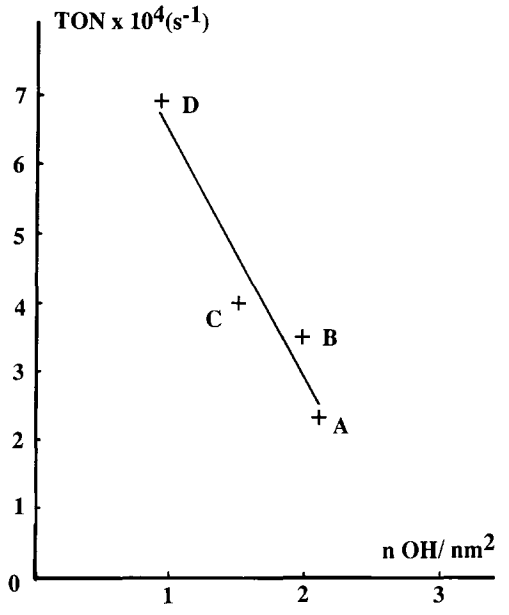

FIG. 12. Turnover number (TON) as a function of the OH density. (TON was defined as the number of isopropanol molecules transformed per second and per OH group).

identification of the hydroxyl groups present on niobium oxide. Infrared bands due to hydroxyl groups were detected at 3710, 3690, 3670, and 3420 cm^{-1} (*36*). The OH groups responsible for the 3420 cm^{-1} band were less stable toward desorption than the three others since they were removed under a treatment under vacuum at 250°C. Temperatures higher than 450°C were needed for the removal of the hydroxyl groups at the origin of the 3710, 3690, and 3670 cm^{-1} bands. From X-ray diffraction measurements, Solid D was found to be constituted of well crystallized $AlNbO_4$. By comparison with the spectra of samples A, B, and C, the spectrum of sample D showed very weak ν OH bands. As a consequence, it can be assumed that the surface of the $AlNbO_4$ solid presents a low coverage of hydroxyl groups.

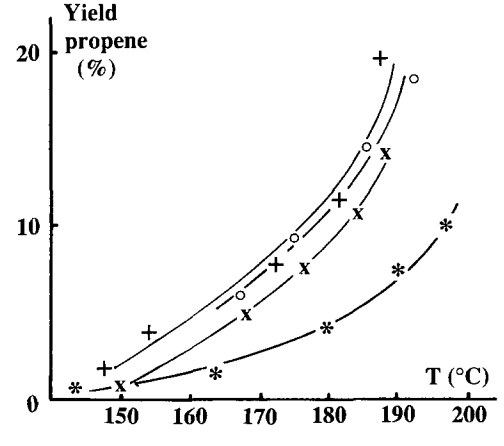

FIG. 11. Catalytic dehydration of isopropanol on AlNbO oxides ○: Solid A; +: Solid B; ×: Solid C; * Solid D (referred to a catalytic mass of 200 mg).

In the case of pure alumina, five types of hydroxyl groups have been detected after calcination under vacuum at elevated temperature, i.e., for around 90% of dehydroxylation. These hydroxyl groups give rise to five well resolved infrared bands after a vacuum treatment at ca. 700°C. They were located at 3800, 3780, 3744, 3733, and 3700 cm^{-1} (*37*). In a later study (*26*), these bands have been assigned to isolated hydroxyl

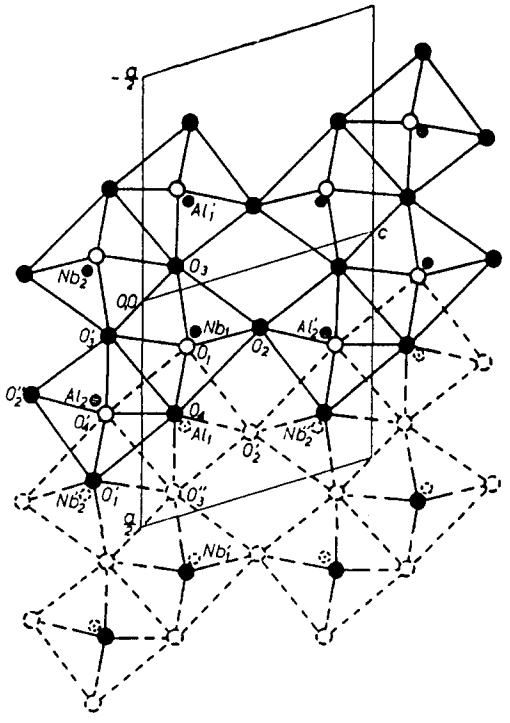

FIG. 13. The structure of $AlNbO_4$ according B. F. Pedersen (*13*). Solid circles indicate atoms situated at $y = 0$. Open circles indicate atoms situated at $y \pm \frac{1}{2}$.

groups surrounded by different numbers of oxygen ions in the (100) surface plane (Table 3). This attribution has been reexamined by Knozinger and Ratnasamy (*38*), assuming that a mixture of low index (111), (110), (100) planes are exposed. Depending on the coordination and the number of aluminum ions bonded to the hydroxyl group, the five ν OH bands have been assigned to OH groups in

TABLE 3

Assignments of the ν OH Bands of Al_2O_3 According to Peri (*37*)

ν OH (cm^{-1})	Number of surrounding oxide ions
3700	0
3730	1
3744	2
3780	3
3800	4

TABLE 4

Assignment of the ν OH Bands of Al_2O_3 According to Knözinger *et al.*(*38*)

ν OH (cm^{-1})	Environment	Net charge/OH
3700–3710	3 Al(Oh)	+0.5
3730–3735	1 Al(Oh) + 1 Al(Td)	+0.25
3740–3745	2 Al(Oh)	0
3760–3780	1 Al(Td)	−0.25
3785–3800	1 Al(Oh)	−0.5

various environments (Table 4). In addition, a net electrical charge was determined for each hydroxyl group. The band with the highest wavenumber (3800 cm^{-1}) was assigned to OH groups having the most negative net charge (−0.5) while the band with the lowest wavenumber (3700 cm^{-1}) corresponds to OH groups having the most positive net charge (+0.5). As a consequence, the OH groups bearing the highest net negative charge are the most basic and behave as the best electron donor group (*38*).

In the infrared spectra of Fig. 7, the band at 3410 cm^{-1} must be attributed to hydroxyl groups bonded to Nb_2O_5 (*36*). The intensity of this band decreases when increasing the calcination temperature, suggesting that the Nb_2O_5 phase disappears in the meantime simultaneously with the Al–Nb–O mixing effect. The absence of the 3410 cm^{-1} band in sample D can be interpreted as the complete disappearance of the Nb_2O_5 phase. The origin of the 3345 cm^{-1} band is later discussed.

The assignment of the other ν OH bands is more complex. First, Nb_2O_5 and Al_2O_3 exhibit infrared absorptions in the same wavenumbers range. Second, the attribution of the alumina ν OH band was performed on solids highly dehydroxylated, whereas the present study was concerned with samples evacuated at only 150°C. In the case of desorptions at moderate temperatures, the alumina shows five ν OH bands at 3790, 3760, 3730, 3685, and 3580 cm^{-1} (*39*). Consequently, the bands at 3730, 3690, and 3580 cm^{-1} of the present study could

be assigned to hydroxyl groups bonded to alumina. The 3790 cm^{-1} band observed on alumina was not present on spectra A, B, and C (Fig. 7). This band was attributed to an hydroxyl group linked to an aluminum atom having an octahedral symmetry. An interaction of this type of OH group with niobia may cause a shift of this band to higher wavenumber. In such a case, the 3820 cm^{-1} band would be assigned to a hydroxyl group of Al_2O_3 pertubed by the presence of niobia. This pertubation may modify the absorption band of surface OH groups of niobia. For instance, some hydroxyl groups at the origin of the 3410 cm^{-1} band that bonded to niobia could interact with alumina; such an interaction could be at the origin of the 3345 cm^{-1} band.

As for Nb_2O_5, the ν OH bands of OH groups linked to alumina progressively disappear when the temperature of calcination increases. This result confirms the formation of a new phase at the expense of niobia and alumina. In the case of the $AlNbO_4$ sample (Solid D), the very weak ν OH bands could be assigned either to $AlNbO_4$ itself or to the presence of small amounts of superficial alumina.

The concentration, nature, and relative intensity of the hydroxyl groups change with calcination temperature. The value of the OH density has been found equal to 0.93 OH/nm^2 for crystalline $AlNbO_4$ (Solid D) which is far from the values usually observed for TiO_2 anatase (4.8 OH/nm^2) and rutile (6.5 OH/nm^2) (*40*). Both FTIR and TGA–MS studies showed a progressive modification of the nature of the surface hydroxyl groups. The presence of Al_2O_3 and Nb_2O_5 structures for low-temperature calcined solids is not detected by XPS measurements. All these results lead us to propose a model for all the AlNbO solids in which Al and Nb are in interaction from the state of the precursor up to the state of the crystalline $AlNbO_4$ phase.

The dehydration of isopropanol on these solids shows an acidic character of the AlNbO oxides. The absence of oxygenates excludes the presence of redox sites which could be expected with Nb. The same activation energy observed for all catalysts suggests that the same type of catalytic dehydrating sites are present. The decrease of the TON with the increasing OH density suggests that inactive OH groups are present at the surface. We can infer from the IR data that OH groups, at the origin of the 3410 cm^{-1} band, are not active in the dehydrating process.

The influence of acidity on reactivity of surface niobium oxide phases, when deposited on Al_2O_3 has yet been demonstrated for methanol oxidation (*41*). Both Lewis and Brønsted surface sites have been taken into account to explain the acidic character which depended highly on the Nb loading. Our AlNbO catalysts, which correspond to a better local dispersion of Nb and Al, appear to be less acidic.

The absence of redox properties for the $AlNbO_4$ support, the presence of different hydroxyl groups bounded to Al and Nb with different acido-basic properties, and the possibility of preparing a material with a high surface without microporosity led us to think that AlNbO oxides should be potential supports for V grafting in comparison with TiO_2 supports. This aspect which is presently under study will be published later.

ACKNOWLEDGMENTS

The authors are indebted to Ms. F. Beauchesne for the electron microscopy characterization of the solids. They thank Dr. J. C. Védrine for fruitful discussion. We acknowledge Conselho Nacional de Desenvolvimento e Pesquisa (CNPq) of Brazil for financial support.

REFERENCES

1. Kung, H. H., "Surface Chemistry and Catalysis," Studies in Surface Science and Catalysis, Vol. 45, p. 20. Elsevier, Amsterdam/Oxford/New York/Tokyo, 1989.
2. Grzybowska, B., *Catal. Today* **1,** 341 (1987).
3. Bond, G. C., and Bruckman, K., *Faraday Discuss. Chem. Soc.* **72,** 235 (1981).
4. Gasior, M., Gasior, I., and Grzybowska, B., *Appl. Catal.* **10,** 87 (1984).
5. Wachs, I. E., Saleh, R. Y., Chan, S. S., and Chersich, C. C., *Appl. Catal.* **15,** 339 (1985).

6. Vejux, A., and Courtine, P., *J. Solid State Chem.* **23,** 93 (1978).
7. Inomata, M., Miyamoto, A., and Murakami, Y., *J. Phys. Chem.* **85,** 2372 (1981).
8. Kozlowski, R., Petifer, R. F., and Thomas, J. M., *J. Phys. Chem.* **87,** 5176 (1983).
9. Haber, J. Machej, T., and Czeppe, T., *Surf. Sci.* **151,** 301 (1985).
10. Eon, J. G., and Courtine, P., *J. Solid State Chem.* **32,** 1 (1985). Papachrysanthou, J., Bordes, E., Vejux, A., Courtine, P., Marchand, R., and Tournoux, M., *Catal. Today* **219,** 1 (1987).
11. Volta, J. C., and Portefaix, J. L., *Appl. Catal.* **18,** 1 (1985).
12. Bond, G. C., and Konig, P., *J. Catal.* **77,** 309 (1982).
13. Pedersen, B. F., *Acta Chem. Scand.* **16,** 421 (1962).
14. Marchand, R., Brohan, L., and Tournoux, M., *Mat. Res. Bull.* **15,** 1129 (1980).
15. Pries de Oliveira, P. G., Eon, J. G., and Volta, J. C., *J. Catal.*, in press.
16. Nakamoto, K., "Infrared Spectra of Inorganic and Coordination Compounds," Wiley, New York, 1970.
17. Muller, M., Thesis, Strasbourg, France, 1970.
18. Burdise and Borlera, *Ric. Sci. Ser.* **3,** 1023 (1963).
19. Moser and Schweiz, *Min. Petrog. Mitt.* **45,** 35 (1965).
20. Pries de Oliveira, P. G., Lefebvre, F., Eon, J. G., and Volta, J. C., *J. Chem. Soc. Chem. Commun.*, 1480 (1990); Pries de Oliveira, P. G., Eon, J. G., and Volta, J. C., *in* "12th Iberoamerican Symposium, Rio de Janeiro, 1990," p. 187. Vol. 2. IBP Edit., Rio de Janeiro, 1990.
21. Engelhardt, G., and Michel, D., "High-Resolution Solid State NMR of Silicates and Zeolites," Wiley, New York, 1987.
22. Gilson, J. P., Edwards, G. C., Peters, A. W., Rajagopalan, K., Wormsbecher, R. F., Roberic, T. G., and Shatlock, M. P., *J. Chem. Soc. Chem. Commun.*, 91 (1987).
23. Samoson, A., Lipmaa, E., Engelhardt, G., Lohse, U., and Jerschkewitz, H. G., *Chem. Phys. Lett.* **134,** 589 (1987).
24. Massiani, P., Chauvin, B., Fajula, F., Figueras, F., and Gueguen, C., *Appl. Catal.* **42,** 105 (1988).
25. Cornelius, E. B., Milliken, T. H., Mills, G. A., and Oblad, A. G., *J. Phys. Chem.* **59,** 809 (1955).
26. Simon, D., Perrin, C., and Baillif, P., *C.R. Acad. Sci. Paris C* **241,** 283 (1976).
27. Mc. Guire, G. E., Schweitzer, G. K., and Carlson, T. A., *Inorg. Chem.* **12,** 2451 (1973).
28. Garbassi, F., Bart, J. C. J., and Petrini, G., J. Elect. Spect. and Rel. Phen., **22,** 95 (1981).
29. Nefedov, V. I., Gati, D., Dzurinskii, D. F., Sergushin, W. P. and Salyn, Y. V., Zh. Neorg. Khim., **20,** 2307 (1975).
30. Lorenz, P., Finster, J., and Wendt, G., *J. Electron Spectrosc. Relat. Phenom.* **16,** 267 (1979).
31. Knozinger, H., *in* "Advances in Catalysis" (D. D. Eley, H. Pines, and P. B. Weisz, Eds.), Vol. 25, p. 184. Academic Press, New York, 1976.
32. Peri, J. B., *J. Phys. Chem.* **69,** 220 (1965).
33. Dunken, H., and Fink, P., *Z. Chem.* **6,** 194 (1966).
34. Zecchina, A., *Discuss. Faraday Soc.* **52,** 89 (1971).
35. Tsyganenko, A. A., and Filimonov, V. N., *J. Mol. Struct.* **19,** 579 (1971).
36. Araujo Gonzalez, W., Nunes, P. P., Lam., Y. L., Guenin, M., Primet, M., and Teichner, S. J., *in* "5th Brasilian Symposium on Catalysis," p. 466. IBP edit., 1989; Araujo Gonzalez, W. Thesis, Military Institute of Engineering, Rio de Janeiro, Brazil, 1991.
37. Peri, J. B., *J. Phys. Chem.* **69,** 211 (1965).
38. Knozinger, H., and Ratnasamy, P., *Catal. Rev. Sci. Eng.* **17,** 31 (1978).
39. Beguin, B., Garbowski, E., and Primet, M., *J. Catal.*, in press.
40. Soenen, V., and Volta, J. C., private communication.
41. Jehng, J.-M., and Wachs, I. E., *Catal. Today* **8,** 37 (1990).